Click Here for Full Article

# Comparison of observed and general circulation model derived continental subsurface heat flux in the Northern Hemisphere

Andrew H. MacDougall,[1,2] Hugo Beltrami,[1] J. Fidel González-Rouco,[3] M. Bruce Stevens,[1,4] and Evelise Bourlon[1]

[1] Heat fluxes in the continental subsurface were estimated from general circulation model (GCM) simulations of the climate of the last millennium and compared to those obtained from subsurface geothermal data. Since GCMs have bottom boundary conditions (BBCs) that are less than 10 m deep and thus may be thermodynamically restricted in the continental subsurface, we used an idealized land surface model (LSM) with a very deep BBC to estimate the potential for realistic subsurface heat storage in the absence of bottom boundary constraints. Results indicate that there is good agreement between observed fluxes and GCM simulated fluxes for the 1780–1980 period when the GCM simulated temperatures are coupled to the LSM with deep BBC. These results emphasize the importance of placing a deep BBC in GCM soil components for the proper simulation of the overall continental heat budget. In addition, the agreement between the LSM surface fluxes and the borehole temperature reconstructed fluxes lends additional support to the overall quality of the GCM (ECHO-G) paleoclimatic simulations.

## 1. Introduction

[2] Simulations of the Earth's climate of the past are key for understanding the behavior of the climate system in a natural state as well as under anthropogenic perturbations. General circulation models' (GCMs) performance simulating the climate of the last millennium provide the metrics on which future climate projections from these GCMs are assessed. By comparing temporal and spatial behaviour of the climate of the past according to GCM simulations against a suite of direct and proxy paleoclimatic data, the confidence of GCM future projections can be interpreted [*Jansen et al.*, 2007; *Randall et al.*, 2007]. However, direct data are spatially and temporally scarce, so most GCMs' performance evaluation is done against proxy data sets, each of which presents particular advantages and disadvantages and thus do not provide a well-constrainted picture of climate indicators for useful comparison.

[3] Recently there have been calls for using energy as a metric [*Hansen et al.*, 2005] of the change in the heat content of Earth's major climate subsystems: the oceans, the atmosphere, the cryosphere, and the continents [*Levitus et al.*, 2001; *Beltrami et al.*, 2002; *Pielke*, 2003; *Levitus et al.*, 2005; *Bindoff et al.*, 2007; *Davin et al.*, 2007]. The heat stored in each of these subsystems is affected by changes in radiative forcing at Earth's surface. Between 1880 and 2003 the average radiative forcing at Earth's surface increased by $1.80 \pm 0.85$ $Wm^{-2}$ [*Hansen et al.*, 2005], causing an increase in the heat content of all of the above subsystems [*Levitus et al.*, 2005; *Bindoff et al.*, 2007]. Estimating the absorption of heat by each subsystem during the second half of the 20th century has been the subject of interest in recent literature [*Beltrami*, 2002b; *Levitus et al.*, 2005; *Keenlyside et al.*, 2008]. An important step in this process is to attempt to examine the performance and limitations of GCMs when modeling the overall energy storage in each of the Earth's climate susbsystems.

[4] The continental subsurface absorbed the largest amount of heat in the second half of the 20th century after the oceans [*Beltrami et al.*, 2002; *Beltrami*, 2002b]. However, the continental subsurface has received little attention in GCM simulations despite important processes occurring at the land-atmosphere interface. A large infusion of heat into the subsurface could destabilize several soil processes, including hydrology [*Zhu and Liang*, 2005; *Bense and Kooi*, 2004], biogeochemical processes such as $CO_2$ production via microbial and root respiration and long-term carbon storage [*Risk et al.*, 2002, 2008; *Kellman et al.*, 2007; *Bekele et al.*, 2007; *Lemke et al.*, 2007; *Diochon and Kellman*, 2008], and permafrost [*Sushama et al.*, 2007; *Lawrence et al.*, 2008]. Each

[1]Environmental Sciences Research Centre, St. Francis Xavier University, Nova Scotia, Canada.
[2]Department of Earth Sciences, Simon Fraser University, Burnaby, British Columbia, Canada.
[3]Departamento de Astrofísica y CC. de la Atmósfera, Universidad Complutense de Madrid, Spain.
[4]Department of Earth Sciences, Dalhousie University, Halifax, Nova Scotia, Canada.

of these processes controls important climate feedback mechanisms and therefore has relevance to the simulation of the whole climate system. In order to project the potential impacts that an increase in heat would have on each of these processes, GCMs must be able to adequately simulate future subsurface heat content.

[5] In this paper we demonstrate the importance of the continental subsurface in Earth's energy budget by a first-order comparison of a GCM-simulated subsurface heat content to the estimates obtained from borehole temperature data. From our results, it is evident that the subsurface model depth in GCMs is typically too shallow to appropriately accommodate simulations that are centuries to a millennium in duration; consequently, GCMs that impose a deeper bottom boundary condition (BBC) yield heat flux values that better compare with measurements.

## 1.1. The Thermal Regime of the Shallow Continental Subsurface

[6] There are two sources of energy fluctuations in the Earth's continental subsurface. The heat derived from the deep interior and surface energy gain (or loss) from the complex energy balance (or imbalance) taking place at the ground surface. The heat from the interior varies on Ma timescales, such that it can be considered constant for climatological purposes. Therefore, the energy balance at the surface determines the variability of the thermal regime of the shallow subsurface.

[7] In conditions without complicating factors such as rapid groundwater movement [*Ferguson et al.*, 2006; *Bense and Beltrami*, 2007], the diffusion of heat into the ground can be described by the one-dimensional time-dependent heat conduction equation:

$$\frac{\partial T}{\partial t} = \kappa \frac{\partial^2 T}{\partial z^2},$$ (1)

where $T$ is temperature, $t$ is time, $z$ is depth (positive downward), and $\kappa$ is thermal diffusivity [*Carslaw and Jaeger*, 1959].

[8] The solution of (1) for a semi-infinite half-space reveals that harmonic temperature oscillations at the surface attenuate with depth and that high-frequency oscillations attenuate faster with depth than low-frequency oscillations [*Smerdon et al.*, 2003, 2004; *Smerdon and Stigelitz*, 2006; *Smerdon et al.*, 2006; *Stieglitz and Smerdon*, 2007]. For typical thermal properties of rock, diurnal signals can be detected only within the first meter below the surface, while annual- and centennial-period signals can be detected down to about 20 and 150 m, respectively [*Beltrami*, 2002a]. Persistent changes in surface temperature penetrate deeper into the ground causing the subsurface to release or absorb heat. Because of the comparatively larger heat capacity of the ground, the subsurface warms and cools much slower than the atmosphere and therefore acts as an energy reservoir.

[9] Because of industrial activities and associated increases in atmospheric greenhouse gases, the energy budget of the Earth is unbalanced [*Hansen et al.*, 2005]. From the thermophysical properties of the ground it is reasonable to expect that the subsurface has absorbed a portion of the energy from this planetary heat imbalance. Geothermal data reveal that the continents absorbed 7 to 9 $\times$ $10^{21}J$ during the latter half of

the 20th century [*Beltrami et al.*, 2002; *Beltrami*, 2002b; *Huang*, 2006]. This magnitude of heat roughly equals that absorbed by the atmosphere over the same time period and is second only in magnitude to the energy absorbed by the oceans [*Levitus et al.*, 2001, 2005; *Bindoff et al.*, 2007].

## 1.2. Energy Balance in Subsurface Models

[10] The thermal regime of the shallow subsurface is determined by a complex series of energy and mass exchanges taking place at the atmosphere-ground interface. Subsurface heat content is important because it drives many physical and biogeochemical processes that are important in the context of present and future climate dynamics, and as a result, all atmosphere-ocean GCMs are coupled to some type of land surface model of varying complexity [*Dirmeyer*, 2000].

[11] A number of recent studies have highlighted the importance of the land-surface component in models for the understanding of climate and climatic variability. *Seneviratne et al.* [2006] used a regional climate model (RCM) to show that land-atmosphere coupling is critical in explaining inter-annual climate variability and that the land surface is crucial to properly project European climate by the middle of the 21st century. Using a similar method, *Fischer et al.* [2007] showed that land-atmosphere coupling must be included in simulations in order to reproduce recent extreme events. Due to the large temperature increase expected in the Arctic during the 21st century and because of the large storage of carbon in permafrost soils, the Arctic has been the prime focus of GCM studies of the subsurface [*Sushama et al.*, 2006; *Stendel et al.*, 2006].

[12] Land-surface models use a mathematical approximation of the one-dimensional heat diffusion equation (1) to simulate diffusion of heat into the subsurface. However, for the boundary value problem to be solved, these algorithms need an imposed value in their deepest layer to bound the approximation. The most common choice of bottom boundary condition (BBC) is the zero-flux condition [*Legutke and Voss*, 1999].

[13] The depth of the BBC is, from a resources and practical point of view, important as shallow BBCs are less computationally intensive. Because GCMs evolved from short-term weather forecast models, typical BBCs in GCMs are located at depths between 1.5 to 10 m [*Smerdon and Stigelitz*, 2006; *Sun and Zhang*, 2004] and thus have important thermodynamical consequences for the shallow subsurface. The effect that shallow BBC placement has on the propagation of heat in the subsurface was the focus of *Lynch and Stieglitz* [1994] showing that, for a snow model, the depth of the subsurface was insufficient to capture annual temperature signals. *Lynch and Stieglitz* [1994] proposed a time-dependent nonzero flux BBC to compensate for the distortion in the annual signal. *Sun and Zhang* [2004] used a conduction based soil model with a zero-flux BBC at a moveable depth and found that a BBC at insufficient depth distorted the annual temperature signal, overestimating subsurface temperatures in the summer and underestimating temperatures in winter by about 2K. More recently *Smerdon and Stigelitz* [2006] investigated the BBC placement problem using analytical solutions to the one-dimensional heat conduction equation for a range of frequencies of temperature oscillations. *Smerdon and Stigelitz* [2006] reported that high-frequency oscillations such as diurnal cycles are not effected by the BBC at depths used in

most GCMs, whereas lower frequency oscillation such as seasonal cycles can be effected in both amplitude and phase up to 100%.

[14] *Stevens et al.* [2007] used a land-surface model to quantify the effect of BBC depth on subsurface heat storage using the mean Northern Hemisphere surface temperature from the ECHO-G's paleoclimatic and future simulations (990–2100 CE) [*González-Rouco et al.*, 2006] as the upper boundary condition. The experiments showed that (1) there is a depth threshold below which the BBC no longer restricts the amount of heat absorbed by the subsurface (this depth, however, is dependent on the length of the simulation) and (2) that a land-surface model with a BBC at a typical depth for a GCM (10 m) absorbs only 25% of the energy absorbed by a land surface model with a deep BBC. The magnitude of the unaccounted heat over the entire continental surface for the 21st century is over an order of magnitude larger than the heat absorbed by the atmosphere or continental surface during the latter half of the 20th century. This quantity of heat may have an effect on physical, biogeochemical, and feedback processes taking place in the soil and shallow subsurface. *Alexeev et al.* [2007] also investigated the effects of BBC placement on temperature in the subsurface and came to similar conclusions as *Stevens et al.* [2007] and *Smerdon and Stigelitz* [2006].

[15] *MacDougall et al.* [2008] examined the problem of limited GCM subsurface heat storage in detail by forcing an idealized finite difference land surface model (FDLSM) with surface temperature output from each of the ECHO-G land-surface grid points. The study showed that when the FDLSM was given the same BBC as ECHO-G total continental heat storage was identical to that in ECHO-G. When a deep BBC was used to bound the FDLSM the difference between the subsurface heat accumulated by ECHO-G and the FDLSM experiment under the A2 (B2) Intergovernmental Panel on Climate Change (IPCC) scenarios was 13 (10) times larger than the difference in subsurface heat storage between the A2 and B2 scenarios in the ECHO-G soil model. This experiment demonstrated that the BBC position is more important in determining subsurface heat storage than the choice of future emissions scenario [*González-Rouco et al.*, 2009; *MacDougall et al.*, 2008].

[16] In this manuscript we estimate the heat storage in the soil model component of a GCM and use the borehole temperature database as a verification field of the GCM derived subsurface heat storage. To estimate subsurface heat content, we use a finite difference land surface model (FDLSM) forced with offline ECHO-G simulated near-surface temperatures as a time-varying upper boundary condition. The FDLSM BBC was placed sufficiently deep (600 m) to ensure that the BBC does not affect the simulated temperatures.

## 1.3. Model and Data Description

[17] The GCM ECHO-G is a coupled-climate model consisting of the atmospheric component ECHAM4 and the ocean component HOPE-G. ECHO-G has 1104 non-glaciated land-surface grid points at a T30 resolution (ca. 3.75° latitude × longitude). The glacial land-surface grid points are not included in subsequent analysis. The ECHO-G soil model has homogeneous and spatially invariant thermal properties across all grid points. It has five vertical layers that increase

in thickness with depth to 9.834 m. The model uses a uniform thermal diffusivity of $\kappa = 7.5 \times 10^{-7}$ m$^2$ s$^{-1}$ and volumetric heat capacity of $\rho_g C_g = 2.4 \times 10^6$ Jm$^{-3}$ K$^{-1}$ [*Legutke and Voss*, 1999].

[18] Here we use the output from two forced 1000 year paleoclimatic simulations for ECHO-G. The two millennial forced simulations (FOR1 and FOR2) differ only in their initial conditions and are driven by the same forcing based on estimates of solar variability, greenhouse gas concentration and stratospheric volcanic aerosols. The FOR1 simulation continues until the end of the 21st century under the IPCC A2 and B2 scenarios. For additional details and extensive model verification of ECHO-G see [*González-Rouco et al.*, 2006, 2009] and references therein.

[19] We use a finite difference land surface model (FDLSM) forced with ECHO-G 0.06 m simulated soil temperatures as a time varying upper boundary. The FDLSM BBC was placed sufficiently deep to ensure changes in surface temperature do not interact with the BBC during the simulation. Comparison of the FDLSM and the ECHO-G soil model component was carried out under a variety of conditions and our results showed that the FDLSM and the ECHO-G soil model component absorb an identical amount of heat and have very similar spatial patterns given the same BBC depth, such that the FDLSM can be used as a proxy for the ECHO-G soil model components in off-line experiments [*MacDougall et al.*, 2008]. The FDLSM was originally designed to study snow-ground thermal interactions and the thermal regime of the subsurface [*Goodrich*, 1982]. As in the ECHO-G simulations, we assume that the dominant heat transfer mechanism in the simulated subsurface is conduction and we used a zero heat flux BBC, such that the bottom boundary is insulated.

[20] The observed continental surface thermal history used in this study was generated from a data set of 588 temperature-depth profiles measured in boreholes from the Northern Hemisphere [*Beltrami et al.*, 2006]. The borehole temperature data are not uniformly distributed, with a higher spatial density in North America and sparser concentration in Eurasia. For this reason fluxes could not be calculated evenly for all regions of the Northern Hemisphere. To avoid giving excessive weight to areas containing large amounts of data, we aggregate the data on a 5° × 5° grid. A block average method was applied to compute a mean location and the L2 norm average value in each cell. This is to suppress redundant data and avoid spatial aliasing [*Smith and Wessel*, 1990]. Rather than a simple arithmetic average, the continental Northern Hemisphere mean flux was estimated using a kilometric gridding, thus cells are of the same size and no area-weighting is required. These sizes were chosen to avoid getting too many cells filled with a single borehole and to have a density as uniform as possible. Grid size effects, however, are not important in the determination of the Northern Hemisphere average [*Pollack and Smerdon*, 2004]. In addition, *González-Rouco et al.* [2006, 2009] have shown, using a comprehensive numerical experiment, that the spatial distribution of present-day borehole data and their sampling frequency between 30°N and 60°N yields a very good representation of the complete Northern Hemisphere past climatic conditions, and the overall continental heat storage values obtained are consistent with estimates obtained with

alternative methods [*Beltrami et al.*, 2002; *Beltrami*, 2002b; *Beltrami et al.*, 2006; *Huang*, 2006].

## 2. Analysis

[21] To test the usefulness of the estimated surface heat fluxes from borehole temperature data as a verification field for GCM simulations, a comparison was made between the surface heat fluxes obtained from the borehole temperature data, ECHO-G simulated soil temperatures, and the off-line FDLSM modeled soil temperatures. The time period of this comparison is 1780–1980, the period for which heat flux estimates from borehole data exist [*Beltrami et al.*, 2006] The change in subsurface heat storage from ECHO-G simulations was calculated using the simulated soil temperatures for the five layers of the soil model component. The heat content was calculated at a monthly resolution for each grid point over all continental areas [*González-Rouco et al.*, 2009; *MacDougall et al.*, 2008] as

$$Q_s = \rho_g C_g \sum_{i=1}^{5} T(i)\Delta z(i), \qquad (2)$$

where $Q_s$ is the subsurface heat storage in $\mathrm{Jm}^{-2}$, $\rho_g C_g$ is the volumetric heat capacity in $\mathrm{Jm}^{-3}\,\mathrm{K}^{-1}$, $T$ is temperature of the layer in K, and $\Delta z$ is the thickness of the layer in m. The change in subsurface heat storage was estimated as the difference in total heat between the initial and the final step of the 1780–1980 period. This process was repeated for all of the continental grid points in ECHO-G under the FOR1 and FOR2 simulations.

[22] The FDLSM was configured with a BBC at a depth of 600 m and thermal properties identical to those used in ECHO-G in the top 10 m and those of typical rock below 10 m. For the rock layer the thermal properties were $\kappa = 1 \times 10^{-6}$ $\mathrm{m}^2$ $\mathrm{s}^{-1}$ and $\rho_g C_g = 3 \times 10^{6}$ $\mathrm{m}^{-3}$ $\mathrm{K}^{-1}$ [*Cermak and Rybach*, 1982]. A BBC depth of 600 m is well beyond the 200–300 m depth *Stevens et al.* [2007] recommends for 200-year simulations, giving our simulations a considerable buffer. The temperatures from the shallowest layer (0.06 m) of the ECHO-G soil model were used as the time varying upper boundary condition of the FDLSM.

[23] The initial thermal state of the subsurface at each grid point was chosen as an isothermal temperature profile, set to the mean temperature of the 0.06 m layer of the ECHO-G soil model for the part of the FOR1 or FOR2 simulation previous to the time period of interest. The FDLSM was allowed to spin-up for several centuries using the 1000–1780 ground-surface temperatures from the ECHO-G simulation as the upper boundary condition. The temperature profile at the end of each spin-up period provided the initial conditions for our experiments. The ECHO-G FOR1 and FOR2 simulations were used at each grid point in nonglaciated continental areas as the time varying upper boundary condition for the FDLSM. At the end of this interval the FDLSM yields the final subsurface thermal state.

[24] The subsurface heat storage in the FDLSM was estimated by the sum of the subsurface temperatures:

$$Q_s = \Delta z \sum_{i=1}^{d-1} \frac{T(i) + T(i+1)}{2} C_v(i), \qquad (3)$$

where $Q_s$ is the subsurface heat storage in $\mathrm{Jm}^{-2}$, $d$ is the total number of discretization intervals (nodes) in the profile, $C_v$ is the volumetric heat capacity in $\mathrm{Jm}^{-3}\,\mathrm{K}^{-1}$, $T$ is the temperature of the layer in $K$, and $\Delta z$ is the internodal spacing in m. The total heat storage was calculated as the difference between the final and initial subsurface thermal states.

[25] For the comparison between the mean surface heat flux from geothermal data and the simulated heat fluxes between 1780 and 1980, the simulated heat accumulations were transformed into mean surface heat fluxes. In order to make the fluxes spatially comparable, the ECHO-G grid was imposed on the flux data. This data were interpolated to a 0.25° longitude × 0.25° latitude grid across much of the Northern Hemisphere. To reduce the resolution of this data the interpolated data point nearest to each ECHO-G grid point was found and every interpolated data point within a 3.75° longitude × latitude box centered at the ECHO-G grid point was averaged to find the mean flux in that cell. This process was repeated for all of the ECHO-G resolved continental nonglaciated grid points. All of the data points outside of the reliable domain of the original data set were masked such that only regions with a sufficient concentration of borehole data for flux reconstructions are shown.

## 3. Results and Discussion

[26] The methodology employed here in these off-line experiments that use the FDLSM as a proxy for an unbounded subsurface does not take into account feedback mechanisms between the land surface and the atmosphere. Therefore, the results from the present experiments are an approximation of the subsurface heat accumulation that a GCM would yield. Similar uncertainties were found by *Lawrence et al.* [2008] in their models of permafrost degradation with shallow and deep BBCs.

[27] Surface flux histories have been retrieved from borehole data from the period 1780–1980 [*Beltrami et al.*, 2006]. Thus we consider the same time period to compare our estimates of subsurface heat storage and surface heat fluxes with those from observations.

[28] Borehole calculated fluxes for this period are shown in Figure 1. Note that flux data are only available over a fraction of the Northern Hemisphere with most of the data concentrated in North America. The average flux for this period in the Northern Hemisphere is 20.6 mW m$^{-2}$ [*Beltrami et al.*, 2006]. Fluxes from the ECHO-G soil model for this time period, for both the FOR1 and FOR2 simulations, are shown in Figure 2. These fluxes are much smaller than observations and have a Northern Hemisphere mean flux of 5.4 mW m$^{-2}$ and 8.6 mW m$^{-2}$ under the FOR1 and FOR2 simulation, respectively (see Table 1).

[29] Surface heat fluxes for the FDLSM experiment with a deep BBC placement are shown in Figure 3 for both the FOR1 and FOR2 simulations. The statistics of these experiments are shown in Table 1. The mean fluxes of both FDLSM experiments are of similar magnitude (22.2 mW m$^{-2}$ under FOR1, and 29.9 mW m$^{-2}$ under FOR2) as the observed mean Northern Hemisphere flux (20.6 mW m$^{-2}$).

[30] The differences between the simulated 600-m FDLSM surface fluxes and observed fluxes are shown in Figure 4. Clearly, the fluxes under the FOR1 scenario are similar over
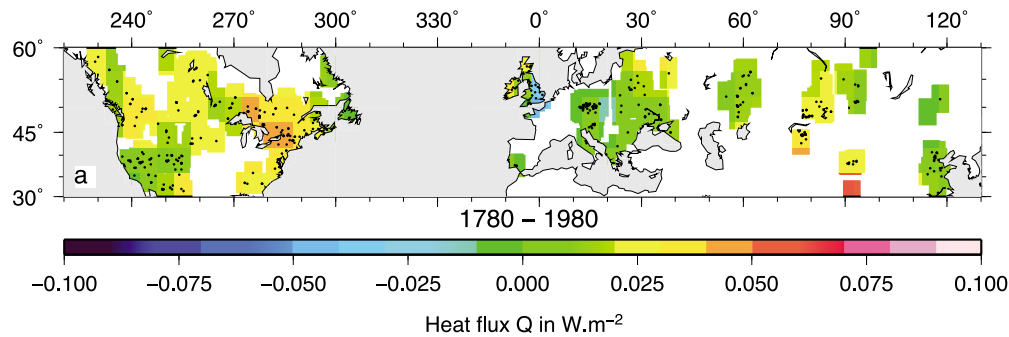
**Figure 1.** Average surface energy flux for 1780–1980 obtained from borehole temperature-depth profiles. Borehole locations are indicated with black dots. Units are in $Wm^{-2}$ [*Beltrami et al.*, 2006].

much of North America, Russia, and China, but the simulated fluxes are too large over much of Europe and the southwestern United States. The FDLSM FOR2 simulation is similar but with a more expansive area of overestimated flux in the same regions (Table 1 for details). Our results indicate that overall simulation of surface heat fluxes by the FDLSM with a deep BBC is in better agreement with the observations than the surface heat fluxes from the ECHO-G simulations with a BBC at 9.83 m. These results accentuate the importance of performing GCM simulations with a deep BBC in the soil model component. In addition, our results show that ECHO-G would produce climatic histories that reasonably reproduce average surface flux history, and subsurface heat storage, when a deep BBC is imposed in the subsurface. That is, these results additionally contribute to validating the performance of ECHO-G's paleoclimatic simulations.

[31] A rough estimate of the possible global surface temperature increase that would occur if all of the energy that could have been absorbed by the deep subsurface was instead reradiated by the surface is about 0.03 K. Such a small increase in global surface temperature is of little consequence to the projections of the change in global surface temperature during the 21st century. This small change would slightly increase the outgoing long-wave flux (Stefan-Boltzmann relationship) and slightly decrease the turbulent heat fluxes which depend on the surface-air thermal gradient. The turbulent fluxes strongly effect evapotranspiration that alters atmospheric emissivity, clouds, and incoming long-wave radiation. These combined feedbacks would impact the model in ways that are nearly impossible to predict without a large-scale GCM simulation experiment. These effects would alter in some way the temperature-time history used to force the FDLSM. Proper estimates of subsurface heat storage will have important consequences for permafrost stability in regions where even a small increase in heat flux could have long-term impacts on active layer thickness. Biogeochemical processes driving the decomposition of organic matter in soils are also strongly dependent on the soil heat content, and a good estimate of subsurface heat would provide guiding principles for long-term soil carbon stability and storage.

[32] Interpreting the agreements and/or discrepancies from the comparison between the borehole-derived subsurface fluxes and the GCM-ECHO-G simulation derived fluxes should be carried out with caution given the uncertainties associated with each of these estimates. The borehole derived
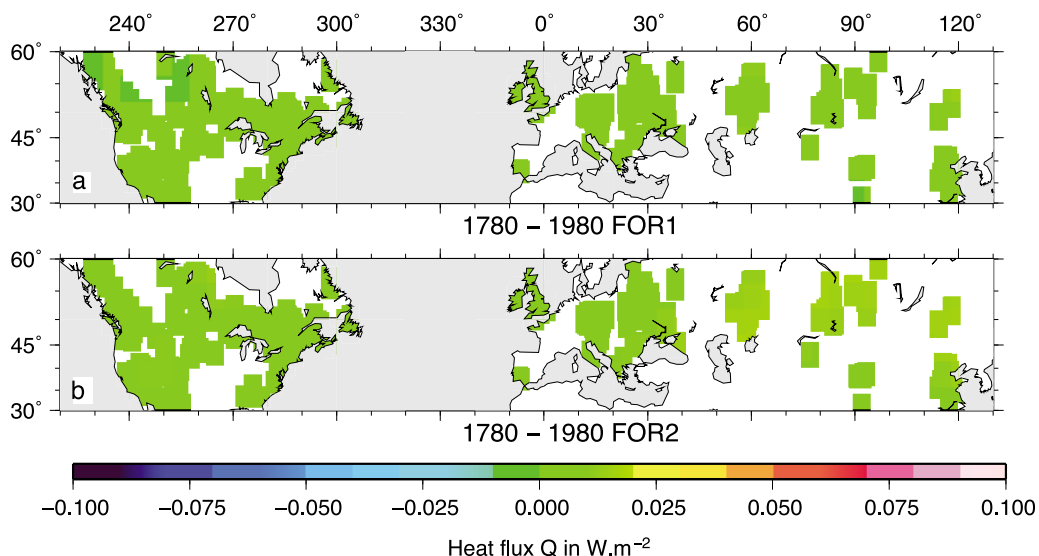


**Figure 2.** Average surface energy flux ($Wm^{-2}$) for 1780–1980 as simulated in the GCM ECHO-G.

**Table 1.** Summary Table of Statistics for the Borehole Reconstructed Surface Flux, ECHO-G Soil Model Surface Flux and the 600-m FDLSM Surface Flux Under the FOR1 and FOR2 Forced Simulations[a,b]

|  | Borehole | ECHO-G | FDLSM | Borehole − ECHO-G | Borehole − FDLSM |
|---|---|---|---|---|---|
|  |  |  | FOR1 |  |  |
| Mean | 20.6 | 5.4 | 22.2 | 13.7 | −1.6 |
| $\sigma$ | 16.4 | 3.3 | 7.9 | 16.9 | 19.3 |
| Min | −59.4 | −2.5 | −0.69 | −63.2 | −79.7 |
| Max | 67.3 | 17.8 | 46.5 | 63.4 | 43.6 |
|  |  |  | FOR2 |  |  |
| Mean | 20.6 | 8.57 | 29.9 | 10.5 | −9.3 |
| $\sigma$ | 16.4 | 3.9 | 10.7 | 17.9 | 21.7 |
| Min | −59.4 | 0.46 | 5.57 | −64.1 | −81.4 |
| Max | 67.3 | 20.0 | 67.7 | 62.2 | 37.2 |

[a]Note. Mean, standard deviation, minimums, and maximums are expressed as mW m$^{-2}$.
[b]Results from the FDLSM have an associated computational error of 2%.

fluxes have uncertainties resulting from the noise present in the geothermal data, from lithological heterogeneities, from differences in the history of land use changes at borehole measurement sites, and from different temperature log data acquisition depth [*Beltrami*, 2002a; *González-Rouco et al.*, 2009]. An approximate error bound on the borehole heat fluxes can be estimated from the differences in subsurface heat accumulation found using independent methods in *Beltrami et al.* [2002] and *Beltrami* [2002b]. These studies found global subsurface heat accumulations that were within 20% of each other. In addition to the data themselves, another source of uncertainty in the borehole subsurface heat fluxes is the effect of the gridding method on the estimated fluxes. Grids that contain many boreholes are more likely to reflect the climate of the entire grid. Grids containing only a small number of boreholes may reflect only a regional climate [*Stevens et al.*, 2008]. This effect is difficult to explicitly quantify and would be best addressed by increasing the spatial coverage of the borehole database.

[33] As demonstrated in this study and earlier works [*Stieglitz and Smerdon*, 2007; *Smerdon and Stigelitz*, 2006; *Stevens et al.*, 2007; *Alexeev et al.*, 2007], the shallow BBC used in GCMs compromises the ability of the models to simulate the correct subsurface thermal field. The shallow BBC problem is here compensated by using the deep BBC FDLSM; however, several additional model simplifications are important to keep in mind when comparing modeled and borehole derived fluxes. The GCM ECHO-G does not include anthropogenic aerosols as a forcing in its millennial simulations, and the lack of these cooling agents may be important, especially in the latter part of our study period. The ECHO-G and the FDLSM both use globally uniform subsurface thermal properties, while the thermal properties of soil and rock vary greatly at the hemispheric scale [*Cermak and Rybach*, 1982]. It is anticipated that nonuniform thermal properties will have a small effect on the simulated hemispheric mean subsurface flux but that the effect may become important at the scale of individual grids. Regional thermal properties can be taken into account using equation (5) below. Carrying out regional scaling is an added layer of complexity that may be explored in future work. Incorporating regionally gridded soil thermal properties may be an important consideration when more sophisticated soil components, which should include a deeper BBC placement, are incorporated into GCMs.

### 3.1. Generality of Results

[34] Throughout this manuscript the thermal properties of the ECHO-G soil model have been used in calculations of heat storage and heat flux. The preceding results are scalable to any set of thermophysical properties. In general, the heat stored in the subsurface $Q$ given a temperature history at the surface $T_0$ is defined by the semi-infinite integral over depth:

$$Q = \rho C \int_0^\infty T(z,t)dz, \qquad (4)$$

where $\rho$ is mass density and $C$ is the volumetric heat capacity of the subsurface. This heat storage from one medium can be
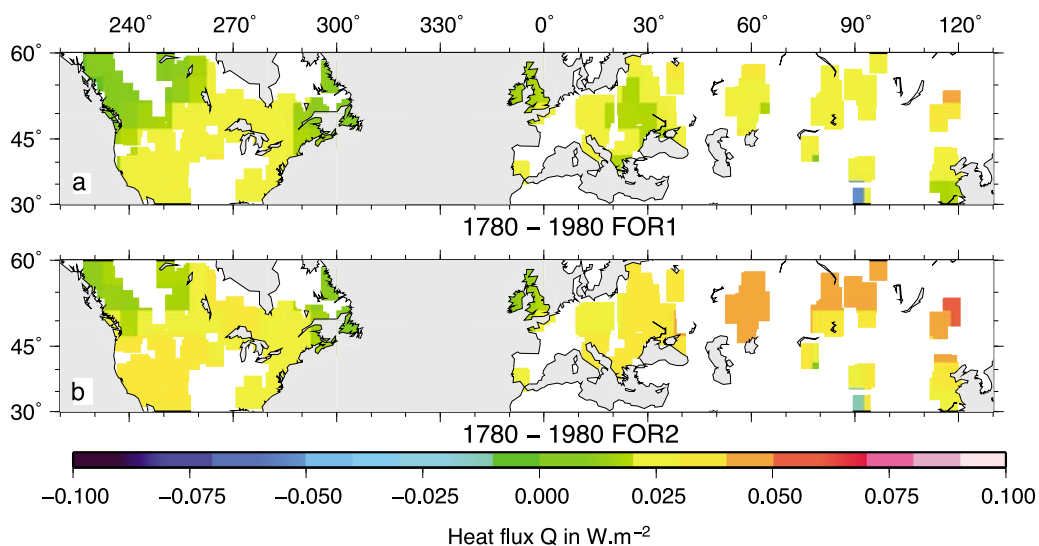


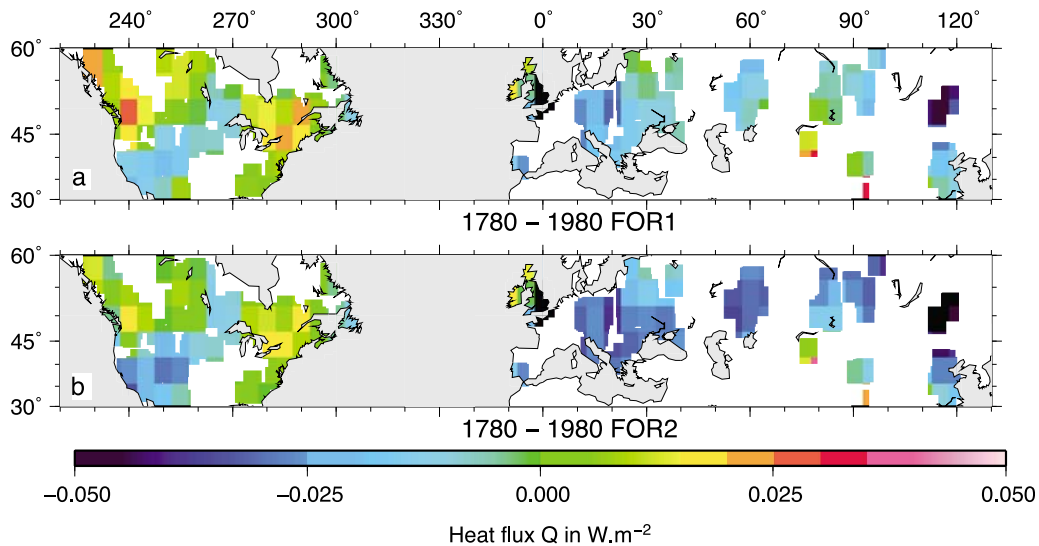**Figure 3.** Average surface energy flux (Wm$^{-2}$) for 1780–1980 as simulated in the offline FDLSM.

**Figure 4.** Difference in average surface flux (Wm$^{-2}$) between borehole temperature reconstructed flux and fluxes for the offline FDLSM.

scaled to a second medium with a different set of properties by the ratio:

$$Q_1 = \frac{\rho_1 C_1 \sqrt{\kappa_1}}{\rho_2 C_2 \sqrt{\kappa_2}} Q_2, \qquad (5)$$

where $Q$, $C$, $\rho$, and $\kappa$ are the heat storage, volumetric heat capacity, density, and thermal diffusivity of subsurfaces 1 and 2, respectively. Equation (5) relates quantities of subsurface (1) to those of subsurface (2) as indicated by subscripts and can also be used to scale subsurface heat fluxes for any set of themophysical properties. As such, regional thermal properties could be used to increase the resolution of surface flux calculations, further enhancing the accuracy of this approach as a verification tool for the subsurface components of GCMs.

## 4. Conclusions

[35] Although it is well known that the continental subsurface hosts a number of temperature-dependent processes that feedback to other climate subsystems and that the subsurface acts as a reservoir for water, carbon, and heat, present-day representation of the subsurface in GCMs is deficient due to the shallow BBCs of their soil model components. This shallow BBC placement distorts the temperature signal in the subsurface, potentially corrupting simulated subsurface processes and preventing large amounts of heat from being absorbed by the subsurface. Permafrost studies have already drawn attention to the shallow depth of the modeled subsurface in GCM and RCM simulations [*Lawrence and Slater*, 2005; *Sushama et al.*, 2007].

[36] The use of a shallow BBC in the GCM ECHO-G has been shown here to compromise the ability of the ECHO-G soil model component to properly simulate surface heat fluxes and subsurface heat absorption. The shallow subsurface model disagrees by more than a factor of 2 with the mean surface heat fluxes obtained for the 1780–1980 period from borehole temperatures. However, the FDLSM forced with ECHO-G near-surface temperatures is able to simulate sur-

face heat fluxes that are in much better agreement with the observations. These results emphasize the importance of placing a deep BBC in GCM soil components for the proper simulation of these heat fluxes. In addition, the agreement between the FDLSM surface fluxes and the borehole temperature reconstructed fluxes lends additional support to the overall quality of the ECHO-G paleoclimatic simulations. The future simulations also show the divergence of the FDLSM simulated subsurface heat absorption from the heat gain in the ECHO-G soil model, with the placement of the BBCs surpassing the thermodynamical effect of the choice of emission scenario as the most important factor determining heat absorption in the simulated subsurface [*MacDougall et al.*, 2008]. The use of surface heat fluxes as a verification field for GCMs requires that deep BBC be used in GCM simulations and that a more complete borehole temperature database be constructed such that fluxes can be resolved over a greater portion of Earth's land surface. Under these conditions borehole temperature records could achieve their potential as a method for validating the long-term, low-fequency climate behavior of GCM paleoclimatic simulations.

## References

Alexeev, V. A., D. J. Nicolsky, V. E. Romanovsky, and D. M. Lawrence (2007), An evaluation of deep configurations in the CLM3 for improved representation of permafrost, *Geophys. Res. Lett.*, *34*, L09502, doi:10.1029/2007GL029536.

Bekele, A., L. Kellman, and H. Beltrami (2007), Soil profile CO2 concentrations variations from forested and clear cut sites in Nova Scotia, Canada, *For. Ecol. Manage.*, *242*, 587–597, doi:10.1016/j.foreco.2007.01.088.

Beltrami, H. (2002a), Earth's long-term memory, *Science*, *297*, 206–207.

Beltrami, H. (2002b), Climate from borehole data: Energy fluxes and temperatures since 1500, *Geophys. Res. Lett.*, *29*(23), 2111, doi:10.1029/2002GL015702.

Beltrami, H., E. Bourlon, L. Kellman, and J. F. González-Rouco (2006), Spatial patterns of ground heat gain in the northern hemisphere, *Geophys. Res. Lett.*, *33*, L06717, doi:10.1029/2006GL025676.

Beltrami, H., J. E. Smerdon, H. N. Pollack, and S. Huang (2002), Continental heat gain in the global climate system, *Geophys. Res. Lett.*, *29*(8), 1167, doi:10.1029/2001GL014310.

Bense, V., and H. Beltrami (2007), The impact of horizontal groundwater flow and localized deforestation on the development of shallow temperature anomalies, *J. Geophys. Res. 112*, F04015, doi:10.1029/2006JF000703.

Bense, V., and H. Kooi (2004), Temporal and spatial variations of shallow subsurface temperature as a record of lateral variations in groundwater flow, *J. Geophys. Res.*, *109*, B04103, doi:10.1029/2003JB002782.

Bindoff, N. L., et al. (2007), Observations: Oceanic climate change and sea level, in *Climate Change 2007: The Physical Science Basis. Contribution of Working Group I to the Fourth Assessment Report of the Intergovernmental Panel on Climate Change*, edited by S. Solomon et al., Cambridge University Press, Cambridge, UK, and New York.

Carslaw, H. S., and J. C. Jaeger (1959), *Conduction of Heat in Solids*, 2nd ed., Oxford University Press, New York.

Cermak, V., and L. Rybach (1982), Thermal conductivity and specific heat of minerals and rocks, in Landolt-Bornstein; Zahlenwerte und Funktionen aus Naturwissenschaften und Technik, edited by G. Angenheister, pp. 305–343, Springer-Verlag, Berlin.

Davin, E. L., N. de Noblet-Ducoudré, and P. Friedlingstein, (2007), Impact of land cover change on surface climate: Relevance of the radiative forcing concept, *Geophys. Res. Lett.*, *34*, L13702, doi:10.1029/2007GL029678.

Diochon, A., and L. Kellman (2008), Natural abundance measurements of 13C indicate increased deep soil carbon mineralization after forest disturbance. *Geophys. Res. Lett.*, *35*, L14402, doi:10.1029/2008GL034795.

Dirmeyer, P. A. (2000), Using a global soil wetness dataset to improve seasonal climate simulation, *J. Clim.*, *13*, 2900–2922.

Ferguson, G., H. Beltrami, and A. Woodbury (2006), Perturbation of ground surface temperature reconstructions by groundwater flow, *Geophys. Res. Lett.*, *33*, L13708, doi:10.1029/2006GL026634.

Fischer, E. M., S. I. Seneviratne, D. Lüthi, and C. Schär (2007), Contribution of land-atmosphere coupling to recent European summer heat waves, *Geophys. Res. Lett.*, *34*, L06707, doi:10.1029/2006GL029068.

González-Rouco, J. F., H. von Storch, and E. Zorita (2003), Deep soil temperature as proxy for surface air-temperature in a coupled model simulation of the last thousand years, *Geophys. Res. Lett.*, *30*(21), 2116, doi:10.1029/2003GL018264.

González-Rouco, J. F., H. Beltrami, E. Zorita, and H. von Storch (2006), Simulation and inversion of borehole temperature profiles in simulated climates: Spatial distribution and surface coupling, *Geophys. Res. Lett.*, *33*, L01703, doi:10.1029/2005GL024693.

González-Rouco, J. F., H. Beltrami, E. Zorita, and M. B. Stevens (2009), Borehole climatology: A discussion based on contributions from climate modeling *Clim. Past Discuss.*, *4*, 1–80.

Goodrich, L. E. (1982), The influence of snow cover on the ground thermal regime, *Can. Geotech. J.*, *19*, 421–432.

Hansen, J., et al. (2005), Earth's energy imbalance: Confirmation and implications, *Science*, *308*, 1431–1435.

Huang, S. (2006), 1851–2004 annual heat budget of the continental landmasses, *Geophys. Res. Lett.*, *33*, L04707, doi:10.1029/2005GL025300.

Jansen, E., et al. (2007), Palaeoclimate, in *Climate Change 2007: The Physical Science Basis. Contribution of Working Group I to the Fourth Assessment Report of the Intergovernmental Panel on Climate Change*, edited by S. Solomon et al., Cambridge University Press, Cambridge, UK, and New York.

Keenlyside, N. S., M. Latif, J. Jungclaus, L. Kornbleh, and E. Roeckner (2008), Advancing decadal-scale climate prediction in the North Atlantic sector, *Nature 453*, 84–88, doi:10.1032/nature06921.

Kellman, L., H. Beltrami, and D. Risk (2007), Changes in seasonal soil respiration with pasture conversion to forest in Atlantic Canada, *Biogeochemistry*, *82*, 101–109, doi:10.1007/s10533–006–9056–0.

Lawrence, D. M., A. G. Slater, V. E. Romanovsky, and D. J. Nicolsky (2008), Sensitivity of a model projection of near-surface permafrost degradation to soil column depth and representation of soil organic matter, *J. Geophys. Res.*, *113*, F02011, doi:10.1029/2007JF000883.

Lawrence, D. M., and A. G. Slater (2005), A projection of severe near-surface permafrost degradation during the 21st century, *Geophys. Res. Lett.*, *32*, L24401, doi:10.1029/2005GL025080.

Lemke, P., J. Ren, R. B. Alley, I. Allison, J. Carrasco, G. Flato, Y. Fujii, G. Kaser, P. Mote, R. H. Thomas, and T. Zhang (2007) Observations: Changes in snow, ice and frozen ground, in *Climate Change 2007: The Physical Science Basis. Contribution of Working Group I to the Fourth Assessment Report of the Intergovernmental Panel on Climate Change*, edited by S. Solomon et al., Cambridge University Press, Cambridge, UK, and New York.

Legutke, S., and R. Voss (1999), *The Hamburg Atmosphere-Ocean Coupled Circulation Model ECHO-G, Tech. Rep., No. 18*, German Climate Computing Center (DKRZ), Hamburg.

Levitus, S., J. Antonov, and T. Boyer (2005), Warming of the world ocean, 1955–2003, *Geophys. Res. Lett.*, *32*, L02604, doi:10.1029/2004GL021592.

Levitus, S, J. I. Antonov, J. L. Wang, T. L. Delworth, K. W. Dixon, and A. J. Broccoli (2001), Anthropogenic warming of Earth's climate system, *Science*, *292*, 5515, 267–270.

Lynch-Stieglitz, M. (1994), The development and validation of a simple snow model for GISS GCM, *J. Clim.*, *7*, 1842–1822.

MacDougall, A. H., J. F. Gonzalez-Rouco, M. B. Stevens, and H. Beltrami (2008), Quantification of subsurface heat storage in a GCM simulation, *Geophys. Res. Lett.*, *35*, L13702, doi:10.1029/2008GL034639.

Meehl, G. A., et al. (2007), Global climate projections, in *Climate Change 2007: The Physical Science Basis. Contribution of Working Group I to the Fourth Assessment Report of the Intergovernmental Panel on Climate Change*, edited by S. Solomon et al., Cambridge University Press, Cambridge, UK, and New York.

Pielke, R. A., Sr. (2003), Heat storage within the Earth system. *Bull. Am. Meteorol. Soc.*, *84*, 331–335.

Pollack, H. N., and J. E. Smerdon (2004), Borehole climate reconstructions: Spatial structure and hemispheric averages, *J. Geophys. Res.*, *109*, D11106, doi:10.1029/2003JD004163.

Randall, D. A., et al. (2007), Climate models and their evaluation, in *Climate Change 2007: The Physical Science Basis. Contribution of Working Group I to the Fourth Assessment Report of the Intergovernmental Panel on Climate Change*, edited by S. Solomon et al., Cambridge University Press, Cambridge, UK and New York.

Risk, D., L. Kellman, and H. Beltrami (2008), A new method for in-situ soil gas diffusivity measurement and applications in the monitoring of subsurface $CO_2$. *J. Geophys. Res.*, *113*, G02018, doi:10.1029/2007JG000445.

Risk, D., L. Kellman, and H. Beltrami (2002), Carbon dioxide in soil profiles: production and temperature dependence, *Geophys. Res. Lett.*, *29*(6), 1087, doi:10.1029/2001GL014002.

Seneviratne, S. I., D. Lüthi, M. Litschi, and C. Schär (2006), Land-atmosphere coupling and climate change in Europe, *Nature*, *443*, doi:10.1038/nature0595.

Smerdon, J. E., H. N. Pollack, V. Cermak, J. W. Enz, M. Kresl, J. Safanda, and J. F. Wehmiller (2004), Air-ground temperature coupling and subsurface propagation of annual temperature signals, *J. Geophys. Res.*, *109*, D21107, doi:10.1029/2004JD005056.

Smerdon, J. E., H. N. Pollack, J. W. Enz, and M. J. Lewis (2003), Conduction-dominated heat transport of the annual temperature signal in soil, *J. Geophys. Res.*, *108*(B9), 2431, doi:10.1029/2002JB002351.

Smerdon, J. E., and M. Stigelitz (2006), Simulation of heat transport in the Earth's shallow subsurface: Lower-boundary sensitivities, *Geophys. Res. Lett.*, *33*, L14402, doi:10.1029/2006GL026816.

Smerdon, J. E., H. N. Pollack, V. Cermak, J. W. Enz, M. Kresl, J. Safanda, and J. F. Wehmiller (2006), Daily, seasonal and annual relationships between air and subsurface temperatures, *J. Geophys. Res.*, *111*, D07101, doi:10.1029/2004JD005578.

Smith, W. H. F, and P. Wessel (1990), Gridding with continuous curvature splines in tension, *Geophysics*, *55*, 293–305.

Stendel, M., V. E. Romanovsky, J. H. Christensen, and T. Sazonova (2006), Using dynamical downscaling to close the gap between global change scenarios and local permafrost dynamics, *Global Planet. Change*, *56*, 203–214.

Stevens, M. B., J. E. Smerdon, J. F. González-Rouco, M. Stieglitz, and H. Beltrami (2007), Effects of bottom boundary placement on subsurface heat storage: Implications for climate model simulations, *Geophys. Res. Lett.*, *34*, L02702, doi:10.1029/2006GL028546.

Stevens, M. B., J. F. González-Rouco, and H. Beltrami (2008) North American climate of the last millennium: Underground temperatures and model comparison, *J. Geophys. Res.*, *113*, F01008, doi:10.1029/2006JF000705.

Stieglitz, M., and J. E. Smerdon (2007), Characterizing land-atmosphere coupling and the implications for subsurface thermodynamics, *J. Clim.*, *20*(1), 21–37.

Sun, S., and X. Zhang (2004), Effect if the lower boundary position of the Fourier Equation on the soil energy balance, *Adv. Atmos. Sci.*, *21*, 868–878.

Sushama, L., R. Laprise, D. Caya, D. Verseghy, and M. Allard (2007), An RCM projection of soil thermal and moisture regimes for North American permafrost zones, *Geophys. Res. Lett.*, *34*, L20711 doi:10.1029/2007GL031385.

Sushama, L., R. Laprise, and M. Allard (2006), Modeled current and future soil thermal regime for northeast Canada, *J. Geophys. Res.*, *111*, D18111, doi:10.1029/2005JD007027.

Zhu, J., and X. Z. Liang (2005), Regional climate model simulations of U.S. soil temperature and moisture during 1982–2002, *J. Geophys. Res.*, *110*, D24110, doi:10.1029/2005JD006472.

A. H. MacDougall, H. Beltrami (corresponding author), E. Bourlon, and M. B. Stevens, Environmental Sciences Research Centre, St. Francis Xavier University, 1 West Street, Antigonish, Nova Scotia B2G 2W5, Canada. (hugo@stfx.ca)

J. F. González-Rouco, Paleoclimate Modeling and Analysis (PalMA), Departamento de Astrofísica y CC. de la Atmósfera, Universidad Complutense de Madrid, Madrid 28040, Spain.